



## OPEN ACCESS

## EDITED BY

Yolande Proroga,  
Experimental Zooprophyllactic Institute of  
Southern Italy (IZSM), Italy

## REVIEWED BY

Guodong Zhang,  
United States Food and Drug Administration,  
United States  
Jorge Velazquez-Roman,  
Autonomous University of Sinaloa, Mexico

## \*CORRESPONDENCE

Fenfen Dong  
✉ 15156874827@163.com

RECEIVED 27 December 2024

ACCEPTED 14 August 2025

PUBLISHED 29 August 2025

## CITATION

Wu X, Chen L, Zhu X, Ji L and Dong F (2025)  
Epidemiological characteristics, virulence  
genes, and antimicrobial resistance analysis of  
*Vibrio parahaemolyticus* in diarrheal cases in  
Huzhou City from 2021 to 2023.  
*Front. Microbiol.* 16:1551984.  
doi: 10.3389/fmicb.2025.1551984

## COPYRIGHT

© 2025 Wu, Chen, Zhu, Ji and Dong. This is  
an open-access article distributed under the  
terms of the [Creative Commons Attribution  
License \(CC BY\)](#). The use, distribution or  
reproduction in other forums is permitted,  
provided the original author(s) and the  
copyright owner(s) are credited and that the  
original publication in this journal is cited, in  
accordance with accepted academic practice.  
No use, distribution or reproduction is  
permitted which does not comply with these  
terms.

# Epidemiological characteristics, virulence genes, and antimicrobial resistance analysis of *Vibrio parahaemolyticus* in diarrheal cases in Huzhou City from 2021 to 2023

Xiaofang Wu, Liping Chen, Xiaojuan Zhu, Lei Ji and  
Fenfen Dong\*

Huzhou Center for Disease Control and Prevention, Huzhou, China

*Vibrio parahaemolyticus* has emerged as a predominant cause of seafood-related infections globally. Despite this, a comprehensive analysis of its epidemiological traits and antimicrobial resistance patterns in Huzhou City remains lacking. Our study isolated 250 strains of *V. parahaemolyticus* from a total of 6,404 diarrhea patients sampled across six hospitals in Huzhou from 2021 to 2023. Epidemiological analysis revealed higher infection rates in warmer seasons, with the majority of cases occurring in individuals aged from 25 to 64. No significant gender-based difference was observed in the prevalence of *V. parahaemolyticus*. Serotype analysis identified O10:K4 as the predominant serotype. 93.20% (233/250) of clinical isolates harbored the *tdh* gene, while 4.0% (10/250) carrying the *trh*. Antimicrobial sensitivity testing indicated a strikingly high resistance rate of 95.56% (172/180) to cefazolin among clinical isolates. The cgMLST-based minimum spanning tree analysis revealed that the O4:KUT clinical isolates segregated into two distinct clusters, ST3 and ST2516, with considerable evolutionary divergence between them. In contrast, the O10:K4 and O3:K6 serotypes exhibited closer phylogenetic proximity. This study comprehensively characterizes *V. parahaemolyticus* in Huzhou, revealing critical insights into its epidemiology, virulence factors, and antibiotic resistance patterns, thereby enhancing our knowledge of its public health risks.

## KEYWORDS

*V. parahaemolyticus*, virulence genes, antibiotic resistance, serovars, epidemiological features

## 1 Introduction

*Vibrio parahaemolyticus* is a Gram-negative, spore-forming bacillus with halophilic properties (Preeprem et al., 2019), widely distributed in coastal areas, marine sediment, and seafood, and is prone to contaminate fish, shrimp, shellfish, and other aquatic products (Zhou et al., 2022). Consumption of undercooked or cross-contaminated food can lead to symptoms such as abdominal pain, diarrhea, acute gastroenteritis, and septicemia. *V. parahaemolyticus* is recognized as a major cause of foodborne disease outbreaks in many Asian countries (Letchumanan et al., 2014). In China, foodborne diseases are mainly caused by pathogenic microorganisms, with outbreaks primarily

caused by *V. parahaemolyticus*, *Salmonella* and *Staphylococcus aureus* (Geng et al., 2019). *V. parahaemolyticus* is one of the most common causative agents of foodborne illness associated with ready-to-eat (RTE) foods (Xie et al., 2016). It is reported that in Zhejiang Province, pathogenic bacteria constitute the primary causative agents of foodborne disease outbreaks, with *V. parahaemolyticus* being the most prevalent species (Chen et al., 2023). Research indicates that *V. parahaemolyticus* has emerged as the leading cause of foodborne diseases in Zhejiang Province, accounting for 58.4% of bacterial outbreaks (Chen et al., 2022). According to statistics, *V. parahaemolyticus* is also one of the main pathogens causing bacterial foodborne outbreaks and sporadic foodborne diarrhea cases in Huzhou City (Yan et al., 2024, 2020). This study selected 250 strains of *V. parahaemolyticus* isolated from sporadic diarrhea cases in at least, from six hospitals of Huzhou City from 2021 to 2023 and used real-time fluorescence PCR and microbroth dilution methods to detect virulence genes, serotypes, and drug sensitivity, in order to understand the epidemiological characteristics, presence of virulence genes, and the current status of antimicrobial resistance of *V. parahaemolyticus* in sporadic diarrhea cases in Huzhou City.

## 2 Materials and methods

### 2.1 Sample collection and *V. parahaemolyticus* serotyping

From January 2021 to December 2023, six hospitals including Wuxing District People's Hospital, Deqing County People's Hospital, Changxing County People's Hospital, Nanxun District People's Hospital, Anji County People's Hospital, and Huzhou First People's Hospital for foodborne disease surveillance in Huzhou City tested 6,404 diarrhea case specimens defined by having a daily bowel movement frequency of  $\geq 3$  times and abnormal stool characteristics (loose stools, watery stools, mucoid stools, or bloody stools, etc.) for *V. parahaemolyticus* (<https://www.who.int/news-room/fact-sheets/detail/diarrhoeal-disease>), and a total of 250 *V. parahaemolyticus* strains were isolated. These included 88 isolations from 2021, 86 isolations from 2022, and 76 isolations from 2023. The number of isolates from each hospital per year was detailed in Table 1. The isolation, identification and serotyping of *V. parahaemolyticus* were performed as previously described (Zhang et al., 2024a). The serotyping of *V. parahaemolyticus* isolates was conducted using standardized slide agglutination assays with commercially available antisera (Denka Seiken Ltd., Tokyo, Japan). The complete serotyping scheme included 11 O (somatic) and 65 K (capsular) antigenic determinants. Isolates were classified into serotypes based on their unique O:K antigen combinations. Isolates that failed to demonstrate K-antigen agglutination were classified as K-untypeable (KUT) serotypes (Jones et al., 2012).

### 2.2 Statistical analysis of temporal distribution of cases

Strain distribution analysis was conducted in Excel according to specimen collection timelines, with data

presentation optimized through bar chart visualization using KaleidaGraph 4.5. The tables were prepared using Microsoft Word.

### 2.3 Virulence gene detection

A fresh bacterial colony was suspended in 200  $\mu$ L sterile water, heat-lysed at 100 °C for 10 min, and centrifuged at 10,000  $\times$  g for 5 min. The DNA-containing supernatant was collected and stored at  $-80$  °C until further use (Yan et al., 2020). Pathogenic *V. parahaemolyticus* can produce either TDH, TRH, or both (Nishibuchi and Kaper, 1995). The gene *tlh* is widely considered to be a marker for *V. parahaemolyticus* (Bej et al., 1999; DePaola et al., 2003). The detection of *tlh*/*tdh*/*trh* virulence genes were performed according to the instructions of the *V. parahaemolyticus* (TLH, TDH, TRH) triplex real-time fluorescent PCR detection kit (Biogen Biological Co., Ltd., Shenzhen, China). The detailed method was performed as previously described (Zhang et al., 2024b). Quality control was performed using the manufacturer-provided negative and positive controls included in the kit to verify test accuracy.

### 2.4 Susceptibility test

In accordance with the Clinical and Laboratory Standard Institution guidelines (CLSI M100-S23) and ChinaPIN-2022-TYJS004, the microbroth dilution method was used to determine the minimal inhibitory concentration (MIC) of *V. parahaemolyticus* against antimicrobial agents. The 13 antimicrobial agents included penicillins: ampicillin (AMP) (64, 32, 16, 8, 4, 2, 1  $\mu$ g/mL), ampicillin/sulbactam (AMS) (64/32, 32/16, 16/8, 8/4, 4/2, 2/1, 1/0.5  $\mu$ g/mL); cephalosporins: cefotaxime (CTX) (16, 8, 4, 2, 1, 0.5, 0.25  $\mu$ g/mL), ceftazidime (CAZ) (32, 16, 8, 4, 2, 1, 0.5  $\mu$ g/mL), cefuroxime (CFX) (32, 16, 8, 4, 2, 1, 0.5  $\mu$ g/mL), cefazolin (CFZ) (32, 16, 8, 4, 2, 1, 0.5, 0.25  $\mu$ g/mL); carbapenems: imipenem (IPM) (8, 4, 2, 1, 0.5, 0.25  $\mu$ g/mL); aminoglycosides: gentamicin (GEN) (32, 16, 8, 4, 2, 1  $\mu$ g/mL); tetracyclines: tetracycline (TET) (32, 16, 8, 4, 2, 1  $\mu$ g/mL); quinolones: nalidixic acid (NAL) (64, 32, 16, 8, 4, 2  $\mu$ g/mL), ciprofloxacin (CIP) (32, 16, 8, 4, 2, 1, 0.5, 0.25, 0.12, 0.06, 0.03, 0.015  $\mu$ g/mL); chloramphenicol: chloramphenicol (CHL) (64, 32, 16, 8, 4, 2  $\mu$ g/mL); and sulfonamides: trimethoprim/sulfamethoxazole (SXT) (8/152, 4/76, 2/38, 1/19, 0.5/9.5, 0.25/4.75  $\mu$ g/mL). The results were expressed as sensitive (S), intermediate (I), and resistant (R). *Escherichia coli* ATCC 25922 was included as a quality control strain.

### 2.5 Statistical analysis

Statistical processing was conducted using SPSS 23.0 software, and data analysis was performed with the chi-square test, with a difference considered statistically significant at  $p < 0.05$ .

TABLE 1 Annual case numbers and positive detection rates from six hospitals in Huzhou City (2021–2023).

Hospitals	2021		2022		2023	
	Cases	Number/ positive detection rate/%	Cases	Number/ positive detection rate/%	Cases	Number/ positive detection rate/%
Huzhou First People's Hospital	482	8/1.66	594	16/2.69	403	5/1.24
Deqing County People's Hospital	197	14/7.11	546	23/4.21	334	15/4.50
Changxing County People's Hospital	244	19/7.79	617	19/3.08	487	32/6.57
Anji County People's Hospital	374	9/2.41	277	9/3.25	238	6/2.52
Wuxing District People's Hospital	387	34/8.79	264	10/3.79	231	6/2.60
Nanxun District People's Hospital	229	4/1.75	254	9/3.54	246	12/4.88
Summary	1,913	88/4.60	2,552	86/3.37	1,939	76/3.92

TABLE 2 Detection of *V. parahaemolyticus* in Huzhou City from 2021 to 2023.

Population Characteristics	2021		2022		2023		Summary	
	Number	Rate (%)	Number	Rate (%)	Number	Rate (%)	Number	Rate (%)
Gender								
Male	985	4.37	1,389	3.02	1,007	3.87	3,381	3.67
Female	928	4.85	1,163	3.78	932	3.97	3,023	4.17
Age								
<5	141	0.00	229	0.00	182	0.00	552	0.00
5–14	79	1.27	121	1.65	117	0.85	317	1.26
15–24	339	1.77	410	2.44	317	4.42	1,066	2.81
25–44	788	5.71	993	3.12	797	4.52	2,578	4.34
45–64	369	6.78	486	7.41	362	5.80	1,217	6.74
≥65	197	5.58	313	2.24	164	2.44	674	3.26

## 2.6 Core genome multilocus sequence typing (cgMLST) profiling and minimum spanning tree-based phylogenetic analysis

We downloaded the 121 sequences of clinical isolates from 2021 to 2023, which were previously submitted to NCBI under BioProject accession numbers PRJNA1115946, PRJNA1072230, and PRJNA1071824 in our prior studies, for subsequent analysis. Detailed strain information was provided in [Supplementary Table S1](#). For the characterization of *V. parahaemolyticus*, seven housekeeping genes (*dnaE*, *gyrB*, *recA*, *dtbS*, *pntA*, *pyrC*, and *tnaA*) were analyzed. A multilocus sequence typing (MLST) scheme was applied to the 121 genomes using *mlst* v2.23.0, generating an MLST profile for each isolate. The *chewBBACA* suite was employed for cgMLST analysis, beginning with schema construction using the *CreateSchema* module ([Silva et al., 2018](#)). Subsequently, allele identification was performed across 95% loci for each isolate through the *AlleleCall* module, producing a 95% allele profile matrix. To maintain analytical rigor, potential paralogous loci were systematically filtered using the *RemoveParalogs* module with default parameters, thereby eliminating sequences that could compromise cgMLST

interpretation. The combination of alleles in each isolate formed an allelic profile that was used to generate minimum spanning trees (MSTs). The MSTs were constructed in *BioNumerics* using the cgMLST allele profiles as input data ([Blanc et al., 2020](#)). The unweighted pair group method with arithmetic mean (UPGMA) was used as the clustering algorithm. The pairwise distance was calculated by counting the number of pairwise allele differences.

## 3 Results

### 3.1 Basic case information

From 2021 to 2023, a total of 6,404 foodborne diarrhea case specimens were collected from six hospitals, yielding 250 isolates of *V. parahaemolyticus*, with an overall positive detection rate of 3.90%. Specifically, in 2021, 1,913 specimens were collected with a positive detection rate of 4.60%. The positive detection rates of Huzhou First People's Hospital, Deqing County People's Hospital, Changxing County People's Hospital, Anji County People's Hospital, Wuxing District People's Hospital, and Nanxun District People's Hospital were 1.66%, 7.11%, 7.79%, 2.41%, 8.79%, and 1.75%, respectively. In 2022, 2,552

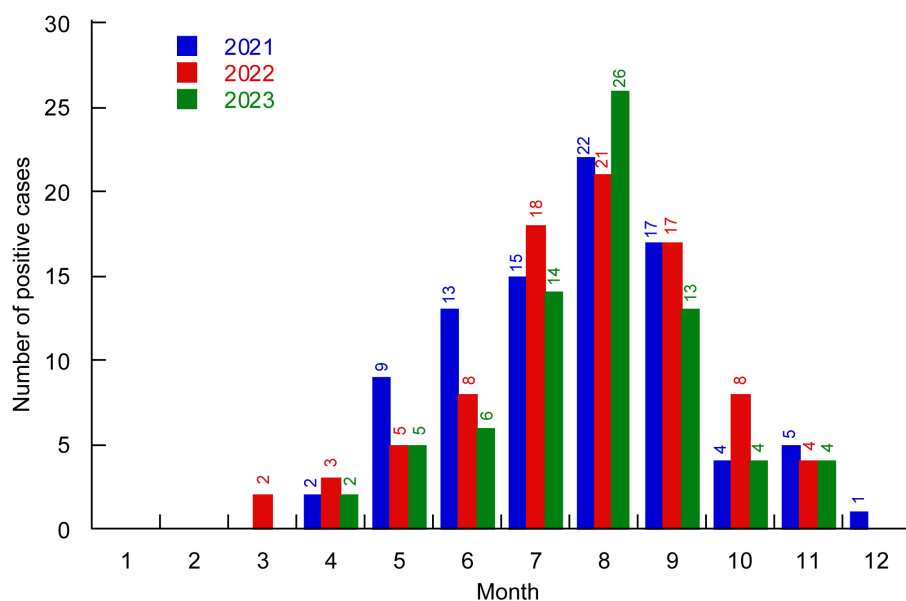


FIGURE 1

Distribution of *V. parahaemolyticus* positive cases in different months of Huzhou City from 2021 to 2023. Different colors represent different years.

specimens were collected with a rate of 3.37%. The positive detection rates for the six hospitals mentioned above were 2.69%, 4.21%, 3.08%, 3.25%, 3.79%, and 3.54%, respectively. In 2023, 1,939 specimens were collected with a rate of 3.92%. The six hospitals reported positive detection rates of 1.24%, 4.50%, 6.57%, 2.52%, 2.60%, and 4.88%, respectively (Table 1). The annual case numbers and positivity rates for the six specific hospitals from 2021 to 2023 are detailed in Table 1. The variation in the detection rate of *V. parahaemolyticus* across the different years was statistically significant ( $\chi^2 = 4.413$ ,  $p < 0.05$ ).

### 3.2 Case population distribution

Among the 6,404 diarrhea infection cases, there were 3381 males and 3023 females.

Positive detection rates of *V. parahaemolyticus* in males and females were 3.67% and 4.17%, respectively, with no statistically significant difference between genders ( $\chi^2 = 0.936$ ,  $p > 0.05$ ). The age distribution of infected cases ranged from 5 months to 97 years, with the highest infection rates in the 45–64 and 25–44 age groups at 6.74% and 4.34%, respectively, and no detection in the age group under 5 years (Table 2). The distribution of detection across different age groups was statistically significant ( $\chi^2 = 59.822$ ,  $p < 0.05$ ).

### 3.3 Temporal distribution of cases

From 2021 to 2023, the detection rate of *V. parahaemolyticus* among foodborne diarrhea patients exhibited a clear seasonal

trend. From March to May (spring), 28 positive cases of *V. parahaemolyticus* were identified from a total of 1,463 samples, resulting in a positive rate of 1.91%. From June to August (summer), 143 positive cases were identified from 2,136 samples, yielding a positive rate of 6.69%. From September to November (autumn), 78 out of 1,709 samples tested positive, with a positive rate of 4.56%. From December to February (winter), only 1 out of 1,096 samples tested positive, with the lowest positive rate of 0.091%. Positive cases were fewer during the winter and spring seasons, peaking in summer and autumn, especially from July to September (Figure 1).

### 3.4 Serovar distribution

Among the 250 *V. parahaemolyticus* strains, 9 O serogroups and 28 serotypes were identified. The most prevalent serovars were O10:K4, constituting 60.00% of the strains (150 out of 250), followed by O3:K6 at 13.20% (33 out of 250), and O4:Kut at 11.20% (28 out of 250). A small fraction, 1.60% (4 out of 250), could not be typed.

In 2021, the strains were distributed across 6 O serogroups and 11 serotypes, with O10:K4 being the most dominant at 81.82% (72 out of 88), followed by O3:K6 at 5.69% (5 out of 88), and O4:Kut at 3.41% (3 out of 88). In 2022, the strains belonged to 5 O serogroups and 12 serotypes, with O10:K4 remaining the most prevalent at 40.70% (35 out of 86), O4:Kut at 27.91% (24 out of 86), and O3:K6 at 13.95% (12 out of 86). In 2023, the strains were categorized into 7 O serogroups and 15 serotypes, with O10:K4 continuing to dominate at 56.68% (43 out of 76), O3:K6 at 21.05% (16 out of 76), and O3:K4 at 3.95% (3 out of 76) (Table 3).

TABLE 3 Serovar distribution of *V. parahaemolyticus* in diarrhea cases in Huzhou city from 2021 to 2023.

O Serogroup	Serotype	2021 (N = 88)		2022 (N = 86)		2023 (N = 76)		Summary	
		Number	Rate (%)	Number	Rate (%)	Number	Rate (%)	Number	Rate (%)
O1	O1:K17	0	0	0	0	1	1.32	1	0.40
	O1:K36	0	0	0	0	1	1.32	1	0.40
	O1:K56	0	0	0	0	1	1.32	1	0.40
	O1:Kut	0	0	2	2.33	0	0	2	0.80
O2	O2:K59	1	1.14	0	0	0	0	1	0.40
O3	O3:K4	0	0	0	0	3	3.95	3	1.20
	O3:K6	5	5.69	12	13.95	16	21.05	33	13.20
	O3:K7	0	0	1	1.16	0	0	1	0.40
	O3:K37	0	0	2	2.33	0	0	2	0.80
	O3:Kut	1	1.14	1	1.16	0	0	2	0.80
O4	O4:K8	0	0	/	/	1	1.32	1	0.40
	O4:K55	1	1.14	2	2.33	0	0	3	1.20
	O4:K61	0	0	0	0	1	1.32	1	0.40
	O4:K63	1	1.14	0	0	0	0	1	0.40
	O4:Kut	3	3.41	24	27.91	1	1.32	28	11.20
O5	O5:Kut	1	1.14	0	0	0	0	1	0.40
O8	O8:K4	0	0	1	1.16	0	0	1	0.40
	O8:K18	0	0	0	0	1	1.32	1	0.40
	O8:K21	0	0	1	1.16	0	0	1	0.40
	O8:Kut	0	0	3	3.49	0	0	3	1.20
O9	O9:K1	0	0	0	0	1	1.32	1	0.40
O10	O10:K4	72	81.82	35	40.70	43	56.58	150	60.00
	O10:K17	0	0	1	1.16	0	0	1	0.40
	O10:K60	1	1.14	0	0	0	0	1	0.40
	O10:K64	0	0	0	0	1	1.32	1	0.40
	O10:Kut	0	0	0	0	1	1.32	1	0.40
O11	O11:K5	1	1.14	0	0	0	0	1	0.40
	O11:Kut	1	1.14	0	0	1	1.32	2	0.80
Untypable		0	0	1	1.16	3	3.95	4	1.60
Summary		88	100.0	86	100.0	76	100.1	250	100.0

### 3.5 Virulence gene detection results

All 250 strains of *V. parahaemolyticus* were identified as carrying the species-specific gene *tlh*. The most common virulence gene profile among these strains was *tdh*+, representing 93.20% of the total; *trh*+ was found in 4.00% of the strains; and the co-presence of both *tdh*+ and *trh*+ was observed in 1.20% (Table 4). We identified four isolates that carried only the *tlh* gene. *tdh*+ strains were predominantly found in serotypes O3:K6, O10:K4, and O4:KUT, whereas *trh*+ and *tdh*+*trh*+ strains were less prevalent among these three major serotypes. *trh*+ strains were distributed across multiple serotypes, including O1:K17, O1:KUT, O2:K59, O4:K63, O8:KUT, O10:K4, O10:K60, O11:K5, and O11:KUT. In

contrast, *tdh*+*trh*+ strains were only detected in O1:KUT, O5:KUT, and O11:KUT.

### 3.6 Susceptibility test results

A random selection of 180 *V. parahaemolyticus* strains were subjected to susceptibility testing. The resistance rate to CFZ was as high as 95.56% (172 out of 180). The resistance rates for other antibiotics were: AMP at 12.78% (23 out of 180), NAL at 3.89% (7 out of 180), AMS and TET at 3.33% (6 out of 180), and CTX and CAZ at 1.11% (2 out of 180). In contrast, all strains were 100.0% sensitive to CFX, IPM, GEN, CHL, CIP, and SXT (Table 5).

TABLE 4 Virulence gene profiles across *V. parahaemolyticus* serotypes in Huzhou from 2021 to 2023.

O serogroup	Serovar	Genotype						Summary	
		<i>tdh</i> <sup>+</sup> <i>trh</i> <sup>-</sup>	Proportion (%)	<i>tdh</i> <sup>-</sup> <i>trh</i> <sup>+</sup>	Proportion (%)	<i>tdh</i> <sup>+</sup> <i>trh</i> <sup>+</sup>	Proportion (%)	Number	Proportion (%)
O1	O1:K17	0	0	1	0.40	0	0	1	0.40
	O1:K36	1	0.40	0	0	0	0	1	0.40
	O1:K56	1	0.40	0	0	0	0	1	0.40
	O1:Kut	0	0	1	0.40	1	0.40	2	0.80
O2	O2:K59	0	0	1	0.40	0	0	1	0.40
O3	O3:K4	2	0.80	0	0	0	0	2	0.80
	O3:K6	33	13.20	0	0	0	0	33	13.20
	O3:K7	0	0	0	0	0	0	0	0
	O3:K37	1	0.40	0	0	0	0	0	0.40
	O3:Kut	2	0.80	0	0	0	0	2	0.80
O4	O4:K8	1	0.40	0	0	0	0	1	0.40
	O4:K55	3	1.20	0	0	0	0	3	1.20
	O4:K61	1	0.40	0	0	0	0	1	0.40
	O4:K63	0	0	1	0.40	0	0	1	0.40
	O4:Kut	28	11.20	0	0	0	0	28	11.20
O5	O5:Kut	0	0	0	0	1	0.40	1	0.40
O8	O8:K4	1	0.40	0	0	0	0	1	0.40
	O8:K18	1	0.40	0	0	0	0	1	0.40
	O8:K21	1	0.40	0	0	0	0	1	0.40
	O8:Kut	2	0.80	1	0.40	0	0	3	1.20
O9	O9:K1	1	0.40	0	0	0	0	1	0.40
O10	O10:K4	149	59.60	1	0.40	0	0	150	60.00
	O10:K17	0	0	0	0	0	0	0	0
	O10:K60	0	0	1	0.40	0	0	1	0.40
	O10:K64	1	0.40	0	0	0	0	1	0.40
	O10:Kut	1	0.40	0	0	0	0	1	0.40
O11	O11:K5	0	0	1	0.40	0	0	1	0.40
	O11:Kut	0	0	1	0.40	1	0.40	2	0.80
Untypeable		3	1.20	1	0	0	0	4	1.60
Summary		233	93.2	10	4.00	3	1.20	246	98.40

### 3.7 Minimum spanning tree analysis

We performed cgMLST analysis on 121 clinical isolates, comprising 85 O10:K4, 15 O3:K6, and 21 O4:KUT strains, and constructed a minimum spanning tree. The results demonstrated that these isolates clustered into two major ST types (ST3 and ST2516) with significant genetic divergence. The O4:KUT serotype was distributed across both ST types. Interestingly, the O10:K4 serotype also separated into two distinct clusters, potentially evolving from O3:K6 strains (Figure 2).

### 4 Discussion

This study analyzed the infection status of *V. parahaemolyticus* in foodborne diarrhea cases in Huzhou City from January 2021 to December 2023, with a positive detection rate of 3.90% among 6,404 diarrhea cases. The detection rate is higher than the average found in Mainland China (2.08%) (Wang et al., 2021), likely attributed to Huzhou’s geographic location and dietary customs. Huzhou City is rich in aquatic products, and its residents have a tradition of consuming raw or undercooked aquatic products. With the development of logistics, various live seafood products



TABLE 5 Antibiotic resistance of *V. parahaemolyticus* in Huzhou from 2021 to 2023.

Categories	Antibiotics	R	I	S
		Number/Rate (%)	Number/Rate (%)	Number/Rate (%)
Penicillins	AMP	23/12.78	56/31.11	101/56.11
	AMS	6/3.33	2/1.11	172/95.56
Cephalosporins	CTX	2/1.11	2/1.11	176/97.78
	CAZ	2/1.11	0/0.00	178/98.89
	CFX	0/0.00	0/0.00	180/100.00
	CFZ	172/95.56	8/4.44	0/0.00
Carbapenems	IPM	0/0.00	0/0.00	180/100.00
Aminoglycosides	GEN	0/0.00	0/0.00	180/100.00
Tetracyclines	TET	6/3.33	0/0.00	174/96.67
Quinolones	NAL	7/3.89	0/0.00	173/96.11
	CIP	0/0.00	0/0.00	180/100.00
Chloramphenicol	CHL	0/0.00	0/0.00	180/100.00
Sulfonamides	SXT	0/0.00	0/0.00	180/100.00

AMP, Ampicillin; AMS, Ampicillin/sulbactam; CTX, Cefotaxime; CAZ, Ceftazidime; CFX, Cefuroxime; CFZ, Cefazolin; IPM, Imipenem; GEN, Gentamicin; TET, Tetracycline; NAL, Nalidixic acid; CIP, Ciprofloxacin; CHL, Chloramphenicol; SXT, Trimethoprim/sulfamethoxazole. R, Resistant; I, Intermediate; S: Susceptible.

are increasingly sold in inland areas. According to the report, the contamination rate of *V. parahaemolyticus* in inland provinces has reached 23.14% (Pang et al., 2020). Therefore, there is a possibility of cross-contamination between seafood and freshwater products during sales and processing (Chen et al., 2021; Liao et al., 2015), leading to infections when people consume contaminated aquatic products.

The temporal distribution shows that *V. parahaemolyticus* infections can occur throughout the year except for January and February, with the majority of cases concentrated in July to September (Huang et al., 2023), which is consistent with the characteristic of high incidence in summer and autumn. According to Zhejiang Meteorological Bureau or Huzhou Meteorological Station reports, from 2021 to 2023, Huzhou experienced significant climatic variability driven by the alternating influences of El Niño-Southern Oscillation (ENSO) phenomena. The extended La Niña conditions (2020–2022) resulted in distinct seasonal patterns, characterized by colder-than-average winter temperatures and increased precipitation variability. Conversely, the emerging El Niño phase in 2023 contributed to intensified summer heatwaves and altered precipitation regimes, consistent with broader warming trends observed across eastern China ([https://epmap.zjol.com.cn/jsb0523/202303/t20230310\\_25510472.shtml](https://epmap.zjol.com.cn/jsb0523/202303/t20230310_25510472.shtml)). High temperatures during these months facilitate bacterial growth and reproduction (Neil et al., 2023; Cantet et al., 2013; Fernandez-Velez et al., 2023). Our study has shown that sporadic diarrhea cases are mainly concentrated in middle-aged and young people (aged 25 to <65 years), which was consistent with previous research (Wang et al., 2021), possibly because this age group has more opportunities to dine out compared to other age groups, and the abundance of night markets in summer and autumn increases the risk of infection when consuming undercooked or raw aquatic products (Li et al., 2020). Consistent with previous findings, the patients aged ≥65

years were the least likely to get infectious diarrhea (Gong et al., 2018). This diversity of age distribution might reflect a natural change in host immunity (Simon et al., 2015) and/or dietary habits that are related to age (Jiang et al., 2024). These findings of the effect of age on the pathogen detection might provide scientific evidence for finding the optimal timing to enhance prevention measures for *V. parahaemolyticus*.

*V. parahaemolyticus* produces thermolabile hemolysin (TLH), thermotolerant direct hemolysin (TDH), and thermotolerant direct hemolysin-related hemolysin (TRH), encoded by the *tlh*/*tdh*/*trh* genes are considered to be key indicators of *V. parahaemolyticus* pathogenicity (Lee et al., 2019; Broberg et al., 2011; Gutierrez West et al., 2013; Shirai et al., 1990). TDH and TRH are considered the most critical virulence factors of *V. parahaemolyticus* (Ceccarelli et al., 2013), with most clinical isolates producing one or both of these hemolysins (Letchumanan et al., 2014). The results of this study show that the positive rate of the *tdh* virulence gene is 93.20%, the *trh* virulence gene is 4.00% and the simultaneous positivity of *tdh* and *trh* virulence genes is 1.20% which was consistent with other study (Sun et al., 2022). Several studies have also reported that around 2.0% of the clinical strains do not contain *tdh* and/or *trh* (Li et al., 2014; Pazhani et al., 2014). Even in the absence of these hemolysins, *V. parahaemolyticus* remains pathogenic indicating that other virulence factors exist (Jones et al., 2012; Mahoney et al., 2010). It was reported that beyond hemolysins, the virulence mechanisms of *V. parahaemolyticus* critically depend on specialized secretion systems that mediate effector delivery into host cells (Orlova, 2015). Notably, the bacterium employs two functionally distinct type III secretion systems (T3SS): T3SS1 facilitates host cell death through the translocation of cytotoxic effectors (VopQ, VopS, VPA0450, and VopR/VP1638), while T3SS2 secretes a distinct repertoire of effectors (VopC, VopT, VopZ, VopA/P, VopV, VopL, and

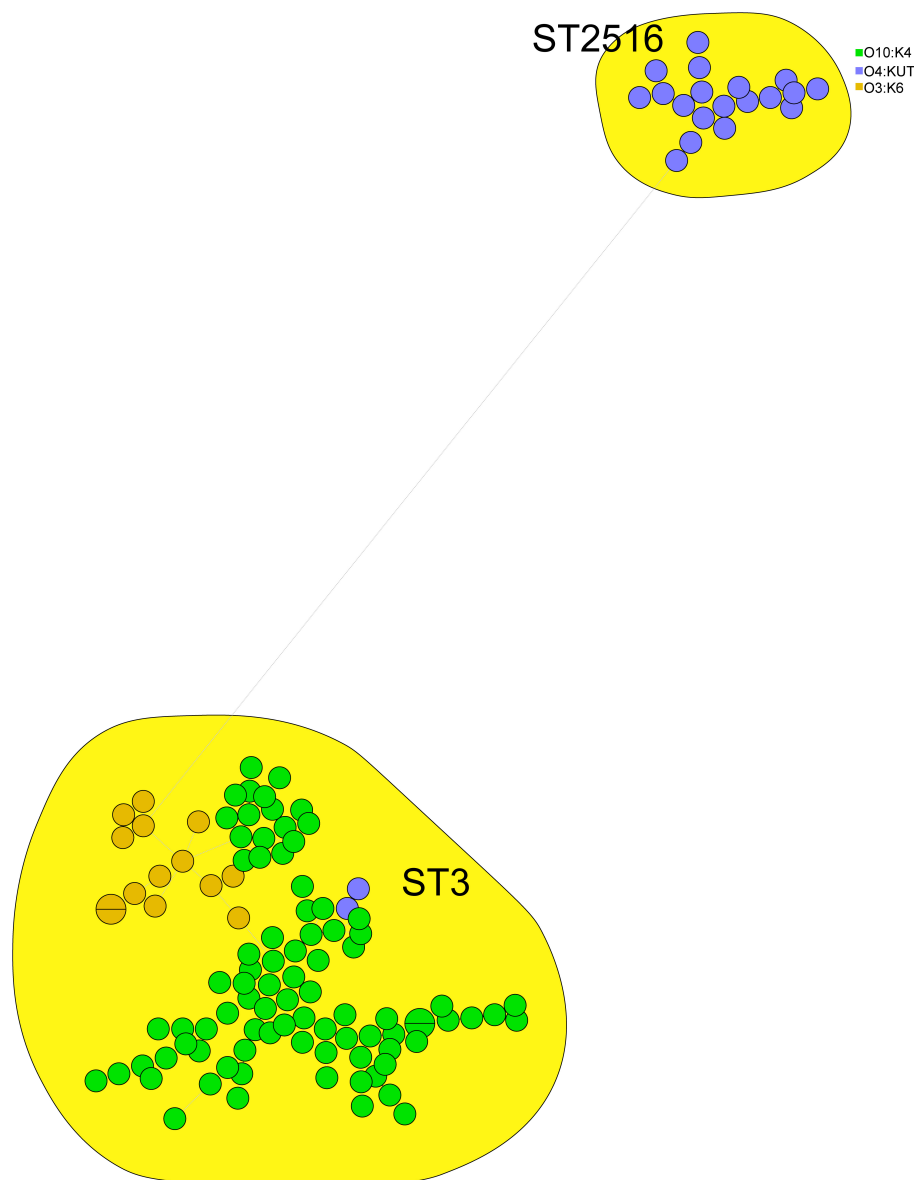


FIGURE 2  
cgMLST based minimum spanning tree of 121 clinical *V. parahaemolyticus* isolates. Circle colors denote different serotypes (O3:K6, O4:KUT, O10:K4), while circle sizes reflect the number of isolates in each node.

VPA1380) that collectively suppress host cell proliferation and induce cytotoxicity (Chatterjee et al., 2013). Additionally, the type VI secretion system (T6SS) contributes to pathogenicity through dual functionality—delivering virulence effectors not only into eukaryotic host cells but also competing bacterial cells (Sha et al., 2013; Li et al., 2019).

In 1996, the O3:K6 serotype of *V. parahaemolyticus* caused a large-scale food poisoning outbreak in India and subsequently became pandemic globally. O3:K6, along with 21 other serotypes, is known as the “pandemic clone” of *V. parahaemolyticus* and is the most frequently reported serotype worldwide (Okuda et al., 1997). Before 2021, the O3:K6 serotype was the main serotype in foodborne diarrhea cases in this region (Zhang et al., 2022). The results of this study show that from 2021 to 2023, the

O10:K4 serotype accounted for 60.00% of foodborne diarrhea cases in Huzhou across all seasons, replacing O3:K6 as the dominant serotype in the region. In fact, in 2020, O10:K4 serotype was detected for the first time in Huzhou City. Afterwards, O10:K4 serotype surpassed O3:K6 as the new dominant serotype (Zhang et al., 2022). In recent years, the O10:K4 serotype has dominated in acute gastroenteritis outbreaks caused by *V. parahaemolyticus* in other provinces in China (Wu et al., 2024; Huang et al., 2022a,b). The emergence of serotype O10:K4 may be the response to host immunologic pressure (Huang et al., 2022a). A previous study indicates that O10:K4 strains and the genetic variant O3:K6 were placed in the same cluster, suggesting a possibility of transfer of the pathogenic genes (Huang et al., 2022b).



With the widespread and extensive use of antibiotics in clinical and breeding fields, the issue of bacterial resistance is becoming increasingly severe. The results of this study show that the resistance rate of *V. parahaemolyticus* to CFZ in Huzhou from 2021 to 2023 was as high as 95.56%; some strains exhibited resistance to AMS, CTX, CAZ, TET, and NAL. The resistance rate of local *V. parahaemolyticus* to CFZ was similar to that of clinical isolates from Nantong (99.1%) and from isolates from Nanjing (99.2%) (Zhou et al., 2022; Huang et al., 2023). However, it was significantly higher than the resistance rate reported for domestic clinical isolates a decade ago (50.4%) (Chen et al., 2016). A previous research has indicated that *V. parahaemolyticus* exhibits a notably high resistance to AMP in recent years (Dahanayake et al., 2020; Lopatek et al., 2018; Mok et al., 2021; Nishino et al., 2021; Vu et al., 2022). However, our study reveals that the organism demonstrates the highest resistance to CFZ, with resistance to AMP at a comparatively lower rate of 12.78%, aligning with previous findings (Zhang et al., 2024a), which may be related to the types of antibiotics used in aquaculture or clinical practice, leading to a decrease in ampicillin resistance. Currently, tetracycline, cephalothin, and quinolone drugs are considered first-line options for the treatment of *V. parahaemolyticus* infections (Elmahdi et al., 2016; Han et al., 2007; Tan et al., 2017). Earlier study reported 100% sensitivity of *V. parahaemolyticus* to the AMS (da Silva et al., 2021), our findings show a concerning development, with 3.33% of strains exhibiting resistance to this antibiotic regimen. The results of this study indicate that, apart from penicillins and cephalosporins, other antibiotics can be used as first-line treatments for *V. parahaemolyticus*. Therefore, continuous resistance monitoring of *V. parahaemolyticus* in foodborne diarrhea cases can timely grasp the trend of resistance changes, which is helpful for guiding rational clinical medication.

In this study, we identified two sequence types (ST3 and ST2516) among 121 clinical *V. parahaemolyticus* isolates (Figure 2). MLST analysis revealed that serotypes O10:K4, O3:K6 and O4:KUT belonged to these two STs, with O4:KUT strains distributed across both ST types and showing significant genetic divergence—a finding consistent with previous reports (Zhang et al., 2024b; Huang et al., 2022a). ST3 emerged as the predominant clinical type, aligning with prior studies that established its clinical significance as an epidemic clone circulating in Asia and America (Chen et al., 2016; Turner et al., 2013). These observations collectively demonstrate the crucial role of ST3 in human infections. Additionally, the O4:KUT strains of ST2516 warrant further investigation due to their potential clinical importance.

In summary, our analysis of *V. parahaemolyticus* infections across six hospitals in Huzhou (2021–2023) revealed that most cases occurred among middle-aged and young adults, with a distinct seasonal concentration during summer months. The predominant serotypes among clinical isolates were O10:K4, O3:K6, and O4:KUT. CgMLST analysis demonstrated significant phylogenetic divergence between some O4:KUT strains and the O10:K4/O3:K6 clusters.

## Data availability statement

The original contributions presented in the study are included in the article/Supplementary material, further inquiries can be directed to the corresponding author.

## Author contributions

XW: Conceptualization, Investigation, Methodology, Software, Writing – original draft. LC: Data curation, Methodology, Writing – original draft. XZ: Methodology, Software, Writing – original draft. LJ: Investigation, Methodology, Software, Writing – review & editing. FD: Investigation, Methodology, Writing – original draft, Writing – review & editing.

## Funding

The author(s) declare that financial support was received for the research and/or publication of this article. This research was funded by the Medical Science and Technology Projects of Zhejiang Province, grant number 2024KY1658 and Natural Science Foundation of Zhejiang Province, grant number LTGY23C010001.

## Conflict of interest

The authors declare that the research was conducted in the absence of any commercial or financial relationships that could be construed as a potential conflict of interest.

## Generative AI statement

The author(s) declare that no Gen AI was used in the creation of this manuscript.

Any alternative text (alt text) provided alongside figures in this article has been generated by Frontiers with the support of artificial intelligence and reasonable efforts have been made to ensure accuracy, including review by the authors wherever possible. If you identify any issues, please contact us.

## Publisher's note

All claims expressed in this article are solely those of the authors and do not necessarily represent those of their affiliated organizations, or those of the publisher, the editors and the reviewers. Any product that may be evaluated in this article, or claim that may be made by its manufacturer, is not guaranteed or endorsed by the publisher.

## Supplementary material

The Supplementary Material for this article can be found online at: <https://www.frontiersin.org/articles/10.3389/fmicb.2025.1551984/full#supplementary-material>

## References

- Bej, A. K., Patterson, D. P., Brasher, C. W., Vickery, M. C., Jones, D. D., Kaysner, C. A., et al. (1999). Detection of total and hemolysin-producing *Vibrio parahaemolyticus* in shellfish using multiplex PCR amplification of *tdh* and *trh*. *J. Microbiol. Methods*, 36, 215–225. doi: 10.1016/S0167-7012(99)00037-8
- Blanc, D. S., Magalhaes, B., Koenig, I., Senn, L., and Grandbastien, B. (2020). Comparison of Whole Genome (wg-) and Core Genome (cg-) MLST (BioNumerics(TM)) Versus SNP Variant Calling for Epidemiological Investigation of *Pseudomonas aeruginosa*. *Front. Microbiol.* 11:1729. doi: 10.3389/fmicb.2020.01729
- Broberg, C. A., Calder, T. J., and Orth, K. (2011). *Vibrio parahaemolyticus* cell biology and pathogenicity determinants. *Microbes Infect.* 13, 992–1001. doi: 10.1016/j.micinf.2011.06.013
- Cantet, F., Hervio-Heath, D., Caro, A., Le Mennec, C., Monteil, C., Quemere, C., et al. (2013). Quantification of *Vibrio parahaemolyticus*, *Vibrio vulnificus* and *Vibrio cholerae* in French Mediterranean coastal lagoons. *Res. Microbiol.* 164, 867–874. doi: 10.1016/j.resmic.2013.06.005
- Ceccarelli, D., Hasan, N. A., Huq, A., and Colwell, R. R. (2013). Distribution and dynamics of epidemic and pandemic *Vibrio parahaemolyticus* virulence factors. *Front. Cell. Infect. Microbiol.* 3:97. doi: 10.3389/fcimb.2013.00097
- Chatterjee, S., Chaudhury, S., McShan, A. C., Kaur, K., De Guzman, R. N. (2013). Structure and biophysics of type III secretion in bacteria. *Biochemistry*. 52:2508–17. doi: 10.1021/bi400160a
- Chen, H., Dong, S., Yan, Y., Zhan, L., Zhang, J., Chen, J., et al. (2021). Prevalence and population analysis of *Vibrio parahaemolyticus* isolated from freshwater fish in Zhejiang Province, China. *Foodborne Pathog. Dis.* 18, 139–146. doi: 10.1089/fpd.2020.2798
- Chen, L., Wang, J., Chen, J., Zhang, R., Zhang, H., Qi, X., et al. (2023). Epidemiological characteristics of *Vibrio parahaemolyticus* outbreaks, Zhejiang, China, 2010–2022. *Front. Microbiol.* 14:1171350. doi: 10.3389/fmicb.2023.1171350
- Chen, L., Wang, J., Zhang, R., Zhang, H., Qi, X., He, Y., et al. (2022). An 11-year analysis of bacterial foodborne disease outbreaks in Zhejiang Province, China. *Foods*, 11:2382. doi: 10.3390/foods11162382
- Chen, Y., Chen, X., Yu, F., Wu, M., Wang, R., Zheng, S., et al. (2016). Serology, virulence, antimicrobial susceptibility and molecular characteristics of clinical *Vibrio parahaemolyticus* strains circulating in southeastern China from 2009 to 2013. *Clin. Microbiol. Infect.* 22, 258e259–216. doi: 10.1016/j.cmi.2015.11.003
- da Silva, L. V., Ossai, S., Chigbu, P., and Parveen, S. (2021). Antimicrobial and genetic profiles of *Vibrio vulnificus* and *Vibrio parahaemolyticus* isolated from the Maryland Coastal Bays, United States. *Front. Microbiol.* 12:676249. doi: 10.3389/fmicb.2021.676249
- Dahanayake, P. S., Hossain, S., Wickramanayake, M., Wimalasena, S., and Heo, G. J. (2020). Manila clam (*Ruditapes philippinarum*) marketed in Korea as a source of vibrios harbouring virulence and beta-lactam resistance genes. *Lett. Appl. Microbiol.* 71, 46–53. doi: 10.1111/lam.13229
- DePaola, A., Nordstrom, J. L., Bowers, J. C., Wells, J. G., and Cook, D. W. (2003). Seasonal abundance of total and pathogenic *Vibrio parahaemolyticus* in Alabama oysters. *Appl. Environ. Microbiol.* 69, 1521–1526. doi: 10.1128/AEM.69.3.1521-1526.2003
- Elmahdi, S., DaSilva, L. V., and Parveen, S. (2016). Antibiotic resistance of *Vibrio parahaemolyticus* and *Vibrio vulnificus* in various countries: a review. *Food Microbiol.* 57, 128–134. doi: 10.1016/j.fm.2016.02.008
- Fernandez-Velez, I., Bidegain, G., and Ben-Horin, T. (2023). Predicting the Growth of *Vibrio parahaemolyticus* in Oysters under varying ambient temperature. *Microorganisms* 11:1169. doi: 10.3390/microorganisms11051169
- Geng, X., Li, W., Zhang, J., Fu, P., Han, H., Liu, J., et al. (2019). [Attribution analysis of food borne disease outbreaks in canteen from 2002 to 2016 in China]. *Wei Sheng Yan Jiu*, 48, 66–69.
- Gong, X. H., Wu, H. Y., Li, J., Xiao, W. J., Zhang, X., Chen, M., et al. (2018). Epidemiology, aetiology and seasonality of infectious diarrhoea in adult outpatients through active surveillance in Shanghai, China, 2012–2016: a cross-sectional study. *BMJ Open* 8:e019699. doi: 10.1136/bmjopen-2017-019699
- Gutierrez West, C. K., Klein, S. L., and Lovell, C. R. (2013). High frequency of virulence factor genes *tdh*, *trh*, and *tlh* in *Vibrio parahaemolyticus* strains isolated from a pristine estuary. *Appl. Environ. Microbiol.* 79, 2247–2252. doi: 10.1128/AEM.03792-12
- Han, F., Walker, R. D., Janes, M. E., Prinyawiwatkul, W., and Ge, B. (2007). Antimicrobial susceptibilities of *Vibrio parahaemolyticus* and *Vibrio vulnificus* isolates from Louisiana Gulf and retail raw oysters. *Appl. Environ. Microbiol.* 73, 7096–7098. doi: 10.1128/AEM.01116-07
- Huang, A., Wang, Y., Xu, H., Jin, X., Yan, B., Zhang, W., et al. (2023). Antibiotic resistance and epidemiology of *Vibrio parahaemolyticus* from clinical samples in Nantong, China, 2018–2021. *Infect. Drug Resist.* 16, 7413–7425. doi: 10.2147/IDR.S432197
- Huang, Y., Du, Y., Wang, H., Tan, D., Su, A., Li, X., et al. (2022a). New variant of *Vibrio parahaemolyticus*, sequence type 3, serotype O10:K4, China, 2020. *Emerging Infect. Dis.* 28, 1261–1264. doi: 10.3201/eid2806.211871
- Huang, Y., Lyu, B., Zhang, X., Tian, Y., Lin, C., Shen, L., et al. (2022b). *Vibrio parahaemolyticus* O10:K4: an emergent serotype with pandemic virulence traits as predominant clone detected by whole-genome sequence analysis—Beijing Municipality, China, 2021. *China CDC Wkly.* 4, 471–477. doi: 10.46234/ccdcw2022.106
- Jiang, D., Han, H., Guo, Y., Zhang, R., Zhan, L., Zhou, Y., et al. (2024). Epidemiological characteristics of sporadic foodborne diseases caused by *Vibrio parahaemolyticus*—China, 2013–2022. *China CDC Wkly.* 6, 1354–1359. doi: 10.46234/ccdcw2024.269
- Jones, J. L., Ludeke, C. H., Bowers, J. C., Garrett, N., Fischer, M., Parsons, M. B., et al. (2012). Biochemical, serological, and virulence characterization of clinical and oyster *Vibrio parahaemolyticus* isolates. *J. Clin. Microbiol.* 50, 2343–2352. doi: 10.1128/JCM.00196-12
- Lee, Y., Choi, Y., Lee, S., Lee, H., Kim, S., Ha, J., et al. (2019). Occurrence of pathogenic *Vibrio parahaemolyticus* in seafood distribution channels and their antibiotic resistance profiles in S. Korea. *Lett. Appl. Microbiol.* 68, 128–133. doi: 10.1111/lam.13099
- Letchumanan, V., Chan, K. G., and Lee, L. H. (2014). *Vibrio parahaemolyticus*: a review on the pathogenesis, prevalence, and advance molecular identification techniques. *Front. Microbiol.* 5:705. doi: 10.3389/fmicb.2014.00705
- Li, L., Meng, H., Gu, D., Li, Y., and Jia, M. (2019). Molecular mechanisms of *Vibrio parahaemolyticus* pathogenesis. *Microbiol. Res.* 222, 43–51. doi: 10.1016/j.micres.2019.03.003
- Li, Y., Xie, T., Pang, R., Wu, Q., Zhang, J., Lei, T., et al. (2020). Food-Borne *Vibrio parahaemolyticus* in China: prevalence, antibiotic susceptibility, and genetic characterization. *Front. Microbiol.* 11:1670. doi: 10.3389/fmicb.2020.01670
- Li, Y., Xie, X., Shi, X., Lin, Y., Qiu, Y., Mou, J., et al. (2014). *Vibrio parahaemolyticus*, Southern Coastal Region of China, 2007–2012. *Emerging Infect. Dis.* 20, 685–688. doi: 10.3201/eid2004.130744
- Liao, Y., Li, Y., Wu, S., Mou, J., Xu, Z., Cui, R., et al. (2015). Risk factors for *Vibrio parahaemolyticus* infection in a Southern Coastal Region of China. *Foodborne Pathog. Dis.* 12, 881–886. doi: 10.1089/fpd.2015.1988
- Lopatek, M., Wiczorek, K., and Osek, J. (2018). Antimicrobial resistance, virulence factors, and genetic profiles of *Vibrio parahaemolyticus* from seafood. *Appl. Environ. Microbiol.* 84, e00537–18. doi: 10.1128/AEM.00537-18
- Mahoney, J. C., Gerding, M. J., Jones, S. H., and Whistler, C. A. (2010). Comparison of the pathogenic potentials of environmental and clinical *vibrio parahaemolyticus* strains indicates a role for temperature regulation in virulence. *Appl. Environ. Microbiol.* 76, 7459–7465. doi: 10.1128/AEM.01450-10
- Mok, J. S., Cho, S. R., Park, Y. J., Jo, M. R., Ha, K. S., Kim, P. H., et al. (2021). Distribution and antimicrobial resistance of *Vibrio parahaemolyticus* isolated from fish and shrimp aquaculture farms along the Korean coast. *Mar. Pollut. Bull.* 171:112785. doi: 10.1016/j.marpolbul.2021.112785
- Neil, W. A., Hard, C., Bowers, J. C., and Jones, J. L. (2023). Levels of *Vibrio parahaemolyticus* in Pacific Oysters (*Crassostrea gigas*) from Washington State following ambient exposure and chilling. *J. Food Prot.* 86:100092. doi: 10.1016/j.jfp.2023.100092
- Nishibuchi, M., and Kaper, J. B. (1995). Thermostable direct hemolysin gene of *Vibrio parahaemolyticus*: a virulence gene acquired by a marine bacterium. *Infect. Immun.* 63, 2093–2099. doi: 10.1128/iai.63.6.2093-2099.1995
- Nishino, T., Suzuki, H., Mizumoto, S., Morinushi, H., Nagaoka, H., Goto, K., et al. (2021). Antimicrobial drug-resistance profile of *Vibrio Parahaemolyticus* isolated from Japanese Horse Mackerel (*Trachurus japonicus*). *Food Saf* 9, 75–80. doi: 10.14252/foodsafetyfscj.D-21-00001
- Okuda, J., Ishibashi, M., Hayakawa, E., Nishino, T., Takeda, Y., Mukhopadhyay, A. K., et al. (1997). Emergence of a unique O3:K6 clone of *Vibrio parahaemolyticus* in Calcutta, India, and isolation of strains from the same clonal group from Southeast Asian travelers arriving in Japan. *J. Clin. Microbiol.* 35, 3150–3155. doi: 10.1128/jcm.35.12.3150-3155.1997
- Orlova, E. V. (2015). A molecular syringe that kills cells. *Nat. Struct. Mol. Biol.* 22, 357–359. doi: 10.1038/nsmb.3021
- Pang, R., Li, Y., Chen, M., Zeng, H., Lei, T., Zhang, J., et al. (2020). A database for risk assessment and comparative genomic analysis of foodborne *Vibrio parahaemolyticus* in China. *Sci Data* 7:321. doi: 10.1038/s41597-020-00671-3
- Pazhani, G. P., Bhowmik, S. K., Ghosh, S., Guin, S., Dutta, S., Rajendran, K., et al. (2014). Trends in the epidemiology of pandemic and non-pandemic strains of *Vibrio parahaemolyticus* isolated from diarrheal patients in Kolkata, India. *PLoS Negl. Trop. Dis.* 8:e2815. doi: 10.1371/journal.pntd.0002815
- Preeprem, S., Singkhamanan, K., Nishibuchi, M., Uddhakul, V., and Mittraparp-Arthorn, P. (2019). Multiplex multilocus variable-number tandem-repeat analysis for

typing of pandemic *Vibrio parahaemolyticus* O1:KUT isolates. *Foodborne Pathog. Dis.* 16, 104–113. doi: 10.1089/fpd.2018.2505

Sha, J., Rosenzweig, J. A., Kozlova, E. V., Wang, S., Erova, T. E., Kirtley, M. L., et al. (2013). Evaluation of the roles played by Hcp and VgrG type 6 secretion system effectors in *Aeromonas hydrophila* SSU pathogenesis. *Microbiology* 159, 1120–1135. doi: 10.1099/mic.0.063495-0

Shirai, H., Ito, H., Hirayama, T., Nakamoto, Y., Nakabayashi, N., Kumagai, K., et al. (1990). Molecular epidemiologic evidence for association of thermostable direct hemolysin (TDH) and TDH-related hemolysin of *Vibrio parahaemolyticus* with gastroenteritis. *Infect. Immun.* 58, 3568–3573. doi: 10.1128/iai.58.11.3568-3573.1990

Silva, M., Machado, M. P., Silva, D. N., Rossi, M., Moran-Gilad, J., Santos, S., et al. (2018). chewBBACA: a complete suite for gene-by-gene schema creation and strain identification. *Microb. Genom.* 4:e000166. doi: 10.1099/mgen.0.000166

Simon, A. K., Hollander, G. A., and McMichael, A. (2015). Evolution of the immune system in humans from infancy to old age. *Proc. Biol. Sci.* 282:20143085. doi: 10.1098/rspb.2014.3085

Sun, J., Li, X., Hu, Z., Xue, X., Zhang, M., Wu, Q., et al. (2022). Characterization of *Vibrio parahaemolyticus* isolated from stool specimens of diarrhea patients in Nantong, Jiangsu, China during 2018–2020. *PLoS ONE* 17:e0273700. doi: 10.1371/journal.pone.0273700

Tan, C. W., Malcolm, T. T. H., Kuan, C. H., Thung, T. Y., Chang, W. S., Loo, Y. Y., et al. (2017). Prevalence and antimicrobial susceptibility of *Vibrio parahaemolyticus* isolated from short mackerels (*Rastrelliger brachysoma*) in Malaysia. *Front. Microbiol.* 8:1087. doi: 10.3389/fmicb.2017.01087

Turner, J. W., Paranjpye, R. N., Landis, E. D., Biryukov, S. V., Gonzalez-Escalona, N., Nilsson, W. B., et al. (2013). Population structure of clinical and environmental *Vibrio parahaemolyticus* from the Pacific Northwest coast of the United States. *PLoS ONE* 8:e55726. doi: 10.1371/journal.pone.0055726

Vu, T. T. T., Hoang, T. T. H., Fleischmann, S., Pham, H. N., Lai, T. L. H., Cam, T. T. H., et al. (2022). Quantification and antimicrobial resistance of *Vibrio parahaemolyticus* in retail seafood in Hanoi, Vietnam. *J. Food Prot.* 85, 786–791. doi: 10.4315/JFP-21-444

Wang, L. P., Zhou, S. X., Wang, X., Lu, Q. B., Shi, L. S., Ren, X., et al. (2021). Etiological, epidemiological, and clinical features of acute diarrhea in China. *Nat. Commun.* 12:2464. doi: 10.1038/s41467-021-22551-z

Wu, X., Zhu, Y., Yan, W., Zhang, P., and Chen, L. (2024). Pathogenic characteristics of the *Vibrio parahaemolyticus* which caused a gastroenteritis outbreak event in Huzhou. *FEMS Microbiol. Lett.* 371:fnad130. doi: 10.1093/femsle/fnad130

Xie, T., Xu, X., Wu, Q., Zhang, J., and Cheng, J. (2016). Prevalence, molecular characterization, and antibiotic susceptibility of *Vibrio parahaemolyticus* from ready-to-eat foods in China. *Front. Microbiol.* 7:549. doi: 10.3389/fmicb.2016.00549

Yan, W., Ji, L., Dong, F., Chen, L., Yuan, R., Zhang, P., et al. (2024). Antimicrobial resistance and genomic analysis of *Vibrio parahaemolyticus* isolates from foodborne outbreaks, Huzhou, China, 2019–2023. *Front. Microbiol.* 15:1439522. doi: 10.3389/fmicb.2024.1439522

Yan, W., Ji, L., Xu, D., Chen, L., and Wu, X. (2020). Molecular characterization of clinical and environmental *Vibrio parahaemolyticus* isolates in Huzhou, China. *PLoS ONE* 15:e0240143. doi: 10.1371/journal.pone.0240143

Zhang, P., Ji, L., Yan, W., Chen, L., Zhu, X., Lu, Z., et al. (2024a). Whole-genome sequencing and transcriptome-characterized mechanism of streptomycin resistance in *Vibrio parahaemolyticus* O10: K4. *Infect. Genet. Evol.* 117:105540. doi: 10.1016/j.meegid.2023.105540

Zhang, P., Wu, X., Ji, L., Yan, W., Chen, L., Lu, Z., et al. (2024b). Prevalence and virulence of *Vibrio parahaemolyticus* isolated from clinical and environmental samples in Huzhou, China. *BMC Genom.* 25:1187. doi: 10.1186/s12864-024-11106-3

Zhang, P., Wu, X., Yuan, R., Yan, W., Xu, D., Ji, L., et al. (2022). Emergence and predominance of a new serotype of *Vibrio parahaemolyticus* in Huzhou, China. *Int. J. Infect. Dis.* 122, 93–98. doi: 10.1016/j.ijid.2022.05.023

Zhou, H., Liu, X., Hu, W., Yang, J., Jiang, H., Sun, X., et al. (2022). Prevalence, antimicrobial resistance and genetic characterization of *Vibrio parahaemolyticus* isolated from retail aquatic products in Nanjing, China. *Food Res. Int.* 162:112026. doi: 10.1016/j.foodres.2022.112026